BMC Neurology

RESEARCH

Open Access

Energy metabolism-related GLUD1 contributes to favorable clinical outcomes of IDH-mutant glioma

Renzhi Deng[1,2,3], Jianying Qin[1,2,3], Lei Wang[1,2,3], Haibin Li[1,2,3], Ning Wen[1,2,3], Ke Qin[1,2,3], Jianhui Dong[1,2,3], Jihua Wu[1,2,3], Dandan Zhu[1,2,3] and Xuyong Sun[1,2,3*]

Abstract

Background Glioma is the most common brain tumor. IDH mutations occur frequently in glioma, indicating a more favorable prognosis. We aimed to explore energy metabolism-related genes in glioma to promote the research and treatment.

Methods Datasets were obtained from TCGA and GEO databases. Candidate genes were screened by differential gene expression analysis, then functional enrichment analysis was conducted on the candidate genes. PPI was also carried out to help determine the target gene. GSEA and DO analysis were conducted in the different expression level groups of the target gene. Survival analysis and immune cell infiltrating analysis were performed as well.

Results We screened 34 candidate genes and selected GLUD1 as the target gene. All candidate genes were significantly enriched in 10 KEGG pathways and 330 GO terms. GLUD1 expression was higher in IDH-mutant samples than IDH-wildtype samples, and higher in normal samples than tumor samples. Low GLUD1 expression was related to poor prognosis according to survival analysis. Most types of immune cells were negatively related to GLUD1 expression, but monocytes and activated mast cells exhibited significantly positive correlation with GLUD1 expression. GLUD1 expression was significantly related to 119 drugs and 6 immune checkpoint genes. GLUD1 was able to serve as an independent prognostic indicator of IDH-mutant glioma.

Conclusion In this study, we identified an energy metabolism-related gene GLUD1 potentially contributing to favorable clinical outcomes of IDH-mutant glioma. In glioma, GLUD1 related clinical outcomes and immune landscape were clearer, and more valuable information was provided for immunotherapy.

Keywords IDH-mutant glioma, GLUD1, Immune microenvironment

*Correspondence:
Xuyong Sun
sunxuyong@gxmu.edu.cn
[1] Transplant Medical Center, The Second Affiliated Hospital of Guangxi Medical University, No.166 Daxuedong Road, Nanning, Guangxi 530007, P.R. China
[2] Guangxi Key Laboratory of Organ Donation and Transplantation, Nanning, Guangxi 530007, P.R. China
[3] Guangxi Transplantation Medicine Research Center of Engineering Technology, Nanning, Guangxi 530007, P.R. China

Introduction

Glioma is most common brain tumorgenerated from glial or precursor cells in central nervous system (CNS) [1]. Low-grade gliomas (LGG) comprise pilocytic astrocytomas, categorized as grade 1, and astrocytomas characterized by the presence of an IDH mutation, classified as grade 2. High-grade gliomas (HGG), on the other hand, consist of astrocytomas with an IDH mutation, designated as grade 3 and 4, as well as glioblastomas (GBM) with an IDH-wildtype status, which are grade 4 malignancies [2]. LGG patients will progress to HGG without effective treatment [3]. The existing treatments are not effective enough because of the complex pathogenesis [4].

Metabolic reprogramming represents a key hallmark of cancerous cells, enabling the sustenance of proliferative signalling, evasion of growth suppressors, and the activation of invasion and metastasis, among other processes [5]. This phenomenon is observed in a range of cancers, [6], including glioma. Metabolic reprogramming is able to shape tumor microenvironment (TME) where tumor cells are more adaptive to grow [7]. Isocitrate dehydrogenase (IDH) plays a critical role in energy metabolism [8] by working in the third reaction in the citric acid cycle. There are two types of IDH in vivo: NADP-dependent IDH (IDH1/2) and NAD-dependent IDH (IDH3) [9]. IDH1/2 mutations have been identified in LGG and HGG, whereas IDH3 mutations don't occur frequently in glioma [10]. Somatic mutations at codon 132 of IDH1 were identified in nearly 12% of HGG [11]. The IDH mutation is related to oncogenesis through the production of 2-hydroxyglutarate which can result in DNA and histone hypermethylation [6], finally inhibits glioma stem cell differentiation and promote TME by upregulating VEGF (vascular endothelial growth factor) [12]. IDH mutation indicates a more favorable prognosis [13]. The aggressiveness increases from LGG-IDH-mutant, LGG-IDH-wildtype, and HGG [14], and recurrence requires shorter time in IDH-wildtype than IDH-mutant glioma [15]. IDH1/2 mutants enzyme inhibitors have been widely applied and shows prospects in research and treatment of glioma [12].

Previous studies have shown that abnormal metabolism leads to different prognoses of patients, and metabolism-related genes can be used as markers of tumor prognosis. A more profound comprehension of the energy metabolism of tumors may help in the development of new treatments [16]. In this study, we aimed to explore energy metabolism-related genes in glioma including different types, in order to provide insights into the pathogenesis and therapy of glioma.

Materials and methods

Data collection

We downloaded mRNA expression profiles and corresponding clinical information from The Cancer Genome Atlas (TCGA) database (https://portal.gdc.cancer.gov/) for TCGA-LGG and TCGA-GBM (GBM meant HGG in "TCGA-GBM") patients, which included a total of 677 glioma samples and 20 normal samples. Samples with incomplete survival information were excluded, leaving 654 patients with complete survival information, including 416 IDH-mutant and 238 IDH-wildtype patients. Also, we downloaded mRNA expression profiles and clinical information of 1018 patients from the CGGA (Chinese Glioma Genome Atlas, http://www.cgga.org.cn/) database for CGGA-693 and CGGA-325 datasets, including 531 IDH-mutant and 435 IDH-wildtype patients.

Furthermore, four datasets were obtained from the Gene Expression Omnibus (GEO) database (https://www.ncbi.nlm.nih.gov/geo/): GSE131273, GSE4290, GSE43378, and GSE31095. GSE131273 comprised 31 glioma samples and 9 normal tissue samples, of which 14 were IDH-wildtype glioma samples and 17 were IDH-mutant glioma samples. GSE4290 included 180 samples, including 81 glioma samples and 23 normal tissue samples. GSE43378 included 50 glioma samples. GSE31095 included 8 glioma samples and 12 normal tissue samples.

Differential gene expression analysis

In this study, we conducted all statistical analyses by R language (version 4.2.1). Differential expression analysis was performed using the "limma" package [17], and differentially expressed genes (DEGs) were filtered with standards of $|\log_2 FC| > 0.5$ and p-value < 0.05.

Functional enrichment analysis

We performed functional enrichment analysis of Gene Ontology (GO) terms, including Biological Process (BP), Molecular Function (MF), and Cellular Component (CC), as well as Kyoto Encyclopedia of Genes and Genomes (KEGG) pathways, using the "clusterProfiler" package [18], by use of DEGs obtained. GO terms and KEGG pathways that were significantly enriched were selected, based on a p-value < 0.05.

Protein–protein Interaction (PPI) analysis

The STRING database [19] (version 11.0) was employed for the analysis and prediction of the functional links and interactions between proteins. The interaction pairs were filtered using a threshold of a minimum required

interaction score > 0.4. Then the PPI network was visualized by Cytoscape [20] (version 3.7.2).

Survival analysis and statistical analyses

The Kaplan–Meier method was employed to estimate the overall survival rate of the various groups, and the significance of differences in survival rates between these groups was assessed using the log-rank test. This analysis was conducted using the "survival" and "survminer" packages (https://CRAN.R-project.org/package=survival). Multivariate Cox regression analysis was utilized to ascertain whether the target gene could predict the survival of patients with IDH-mutant glioma.

The "oncoPredict" package [21] was utilized to conduct drug sensitivity prediction. Wilcoxon rank-sum test was performed to compare gene expression and immune cell infiltration differences between different groups. The "cor" function was used to perform Pearson correlation analysis. Differences were deemed statistically significant when $p < 0.05$.

Origin of Cell Lines

The cell lines employed in this experiment included normal human astrocytes (HA1800) and human glioblastoma cells (H4, U251, A172), all of which were procured from the National Infrastructure of Cell Line Resources (http://www.cellresource.cn/). The cells were cultured in Dulbecco's Modified Eagle Medium (DMEM) with high glucose (C11995500BT, Grand Island Biological Company (Gibco), Waltham, MA, US), supplemented with a 1% penicillin–streptomycin (P/S) mixture and 10% fetal bovine serum(FBS) (10,099–141, Gibco). The cell cultures were maintained at 37 °C in a humidified incubator with 5% CO_2.

Quantitative Reverse Transcription Polymerase Chain Reaction (qRT-PCR)

Total RNA was extracted from the cells using TRNzol Universal Total RNA Extraction Reagent (DP424, Tiangen Biotech (Beijing) Co., Ltd., Beijing, China). The integrity of the RNA was evaluated through 1.5% agarose gel electrophoresis, and its purity and concentration were determined using NanoDrop 2000. Reverse transcription was conducted using the RevertAid First Strand cDNA Synthesis Kit (K1622, Thermo Fisher Scientific, Waltham, MA, US). For qPCR experiments, the TB Green® Premix Ex Taq™ II (Tli RNaseH Plus) kit (RR820A, Takara Biomedical Technology (Beijing) Co., Ltd., Beijing, China) wasutilized, with the subsequent detection occurring on an RT-PCR system (StepOne Plus, Applied Biosystems, Waltham, MA, US). The program involved an initial denaturation at 95 °C for 30 s, followed by 40 cycles of denaturation at 95 °C for 5 s and annealing/extension at 60 °C for 30 s. GAPDH served as the reference gene, and the primer sequences are provided in Table 1. Each sample was tested in triplicate, and mRNA expression levels were determined using the $2^{-\Delta\Delta CT}$ method.

Western Blot (WB)

Following the extraction of protein using Radioimmunoprecipitation assay (RIPA) lysis buffer and Phenylmethylsulfonyl fluoride (PMSF), protein concentrations were quantified using the BCA protein quantification kit (CW0014S, Jiangsu Cowin Biotech Co.,Ltd, Taizhou, Jiangsu, China). The following protocol was conducted in accordance with the methodology previously outlined [22]. A primary antibody against GLUD1 (TA376611, 1:1000) was purchased from OriGene Technologies, Inc. (Rockville, MD, US), and a primary antibody against GAPDH (60,004–1-Ig, 1:50,000) was obtained from Proteintech Group, Inc. (Rosemont, IL, US). Both primary antibodies were detected using a secondary antibody of horseradish peroxidase (HRP)-labeled goat anti-mouse IgG (H + L) (ZB-2305, 1:10,000) from Beijing Zhong Shan-Golden Bridge Biological Technology Co., Ltd. (Beijing, China). Finally, the band intensities were analyzed using the Image J software.

Gene Set Enrichment Analysis (GSEA) and Disease Ontology (DO) analysis

Using "limma" package, the expression levels of the target genes were grouped based on their median expression levels. Samples exhibiting expression levels exceeding the median were categorized as the high-expression group, whereas those displaying expression levels below the median were designated as the low-expression group. Differential expression analysis was performed between the two groups. The "clusterProfiler" package [18] was used to perform GSEA analysis between the two groups, with significant pathway enrichment defined as

Table 1 Primer sequences for qRT-PCR

Genes	Forward Primer (5′-3′)	Reverse Primer (5′-3′)	Product length (bp)
GAPDH	GAAGGTGAAGGTCGGAGTC	GAAGATGGTGATGGGATTTC	227
GLUD1	TTTGGTGCTAAATGTATTGCTGTTG	ATAGGGCTTTGCCTTGGGG	135

p-value < 0.05. The "DOSE" package [23] was used to perform pathway enrichment analysis based on the differential expression analysis results.

Calculation of infiltration ratios of immune cells

The relative proportions of 22 immune cell types were calculated in the samples using the software CIBERSORT [24] Xcell (https://xcell.ucsf.edu/) and TISIDB (http://cis.hku.hk/TISIDB/) databases were used to calculate the abundance of immune cells. The "estimate" function package (https://R-Forge.R-project.org/projects/estimate/) was used to calculate the immune scores of the samples.

Results

Differentially expressed energy metabolism-related genes between IDH wild-type and IDH-mutant glioma

Energy metabolism-related gene sets (REACTOME_METABOLISM_OF_AMINO_ACIDS_ AND_DERIVATIVES, REACTOME_METABOLISM_OF_CARBOHYDRATES, and REACTOME_METABOLISM_OF_LIPIDS) were downloaded from MSigDB (version 7.0; http://software.broadinstitute.org/gsea/msigdb/), resulting in a total of 1384 genes (Table S1). Based on these genes, differential expression analysis was performed between IDH-wildtype and IDH-mutant glioma using the TCGA dataset. A total of 179 differentially expressed energy metabolism-related genes were identified (Table S2), including 55 upregulated genes and 124 downregulated genes in the IDH-mutant group (Fig. 1A). Principal component analysis (PCA) indicated that IDH-wildtype and IDH-mutant glioma samples could be separated (Fig. 1B). Kaplan–Meier survival analysis between the two groups showed that patients with IDH-mutant glioma had a better prognosis (Fig. 1C).

Differential expression analysis was also performed on the GSE4290 dataset, comparing GBM samples (all GBM samples were IDH-wildtypes) to normal samples, resulting in a total of 8221 DEGs (GBM onset related genes, GRGs), including 4772 upregulated genes and 3449 downregulated genes (Fig. 1D). We also performed differential expression analysis between IDH-wildtype glioma and IDH-mutant glioma from the GSE131273 dataset as well, resulting in a total of 6490 DEGs (IDH-mtRGs), including 3569 upregulated genes and 2921 downregulated genes in IDH-mutant glioma (Fig. 1E).

The GRGs and IDH-mtRGs were intersected with the differentially expressed energy metabolism-related genes obtained from TCGA database, resulting in 34 candidate genes (Fig. 1F, Table S3). GO and KEGG enrichment analysis was performed on these genes. There were 10 significantly enriched KEGG pathways (p-value < 0.05) (Fig. 1G), 247 significantly enriched BP terms, 59 significantly enriched MF terms, and 24 significantly enriched CC terms (top ten were shown in Fig. 1H). Interestingly, they were highly related to extracellular matrix (ECM) and enzymes generating ECM. In GLUD1 transgenic mice, several extracellular matrix interacting genes were also upregulated [25]. Detailed results of the enrichment analysis were attached in Table S4.

Low expression of energy metabolism-related gene GLUD1 was associated with poor prognosis in IDH-mutant glioma samples

To further confirm the hub genes among the candidate genes, we constructed a PPI network based on 34 candidate genes using the STRING database (Fig. 2A), and we selected GLUD1 as our target gene for further study, considering large differential significance and the scarcity of previous research on GLUD1.

We analyzed the expression of GLUD1 in glioma vs. control samples using the GSE31095 dataset, and found that GLUD1 was downregulated in glioma samples (Fig. 2B). GLUD1 expression was higher in IDH-mutant than in IDH-wildtype samples (Fig. 2C). The expression of GLUD1 in different grades of glioma was also analyzed using the CGGA database showing that GLUD1 expression decreased with increasing grade (Fig. 2D). Furthermore, we found that GLUD1 expression of IDH-mutant glioma samples significantly decreased from low to high grades (Fig. 2E).

TIMER database was also used to analyze the expression of GLUD1 in various cancers. The results showed that GLUD1 expression was significantly downregulated in multiple tumors, like BLCA (bladder urothelial carcinoma), BRCA (breast invasive carcinoma), and other tumor samples (Fig. 2F). We then validated the expression of GLUD1 in tumor and normal tissues using the HPA database (https://www.proteinatlas.org/) and found that GLUD1 expression was lower in tumor tissues than in normal tissues (Fig. 2G). We also performed qRT-PCR (Fig. 2H) and WB (Fig. 2I) to validate the expression of GLUD1. Both results showed that GLUD1 was expressed at significantly lower levels in glioma cell lines than in normal cells.

We divided IDH-mutant samples in the TCGA dataset into high and low expression groups ($GLUD1^{high}$ group, $GLUD1^{low}$ group) based on the optimal cutoff value for GLUD1, and performed KM survival analysis. The results showed that patients in $GLUD1^{low}$ group had a relatively poor prognosis, whether in HGG or LGG (Fig. 3A-C). The same result also occurred in GSE43378 dataset with the grouping standard of median GLUD1 expression (Fig. 3D). In HGG and LGG, the survival probability of $GLUD1^{high}$ group was higher than $GLUD1^{low}$ group (Fig. 3E-F).

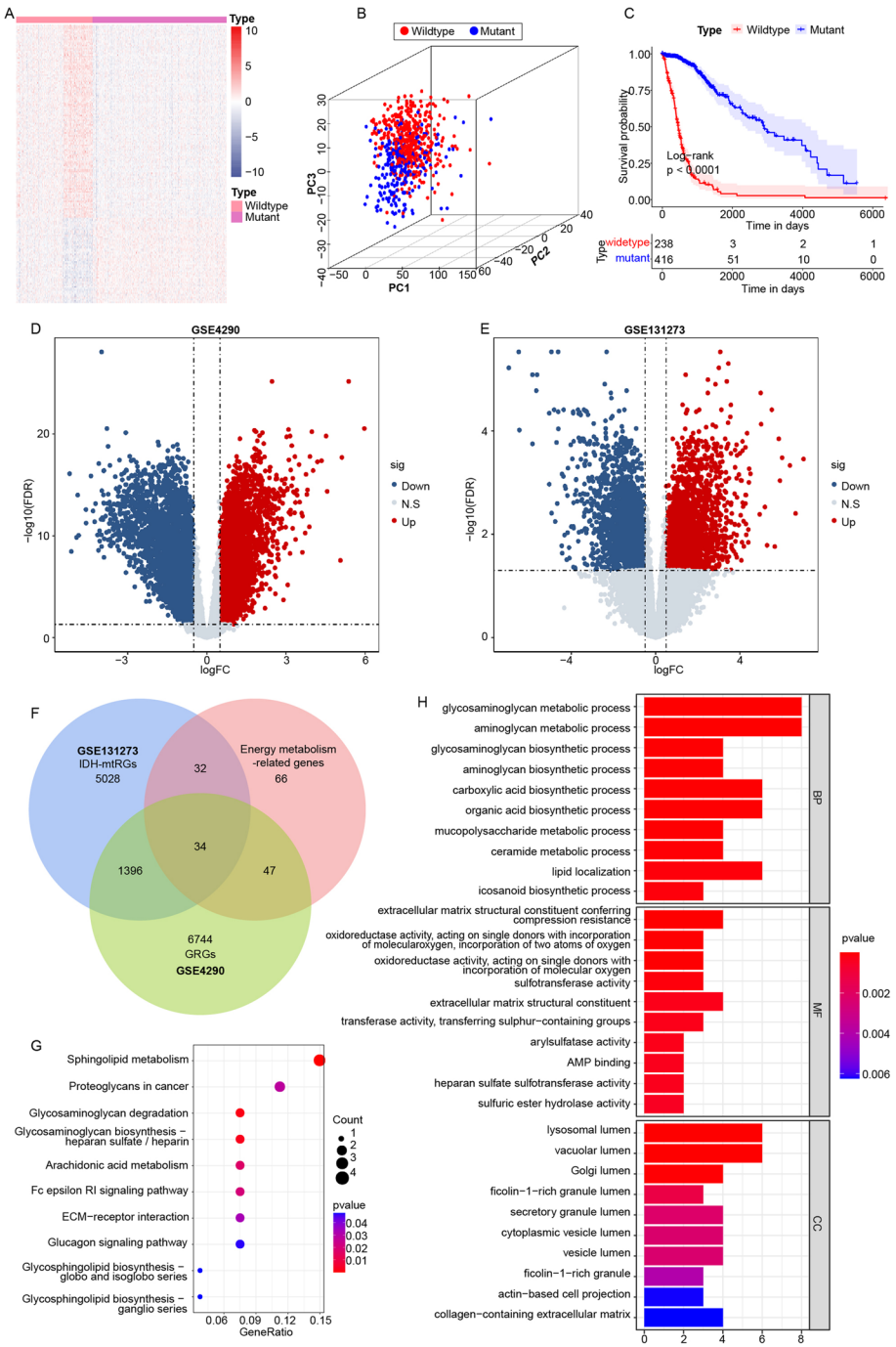

Fig. 1 Differentially expressed energy metabolism-related genes between IDH wild-type and IDH-mutant glioma. **A** Differential gene expression in TCGA dataset. **B** PCA analysis of IDH wild-type and IDH-mutant glioma groups. **C** Kaplan–Meier survival analysis between IDH wild-type and IDH-mutant glioma groups. **D**-**E** Differential expression analysis in GSE4290 and GSE131273 datasets. **F** Determination of candidate genes. **G**-**H** Top 10 significantly enriched KEGG pathways and GO terms (BP, MF, CC)

Functions and pathways affected by key energy metabolism-related gene GLUD1 in IDH-mutant glioma

Due to the higher survival rate in IDH-mutant glioma patients (Fig. 1C) and the higher expression in IDH-mutant samples (Fig. 2D), it was necessary to explore the potential functions and pathways affected by GLUD1 in IDH-mutant glioma. GSEA analysis was performed on IDH-mutant samples in the TCGA

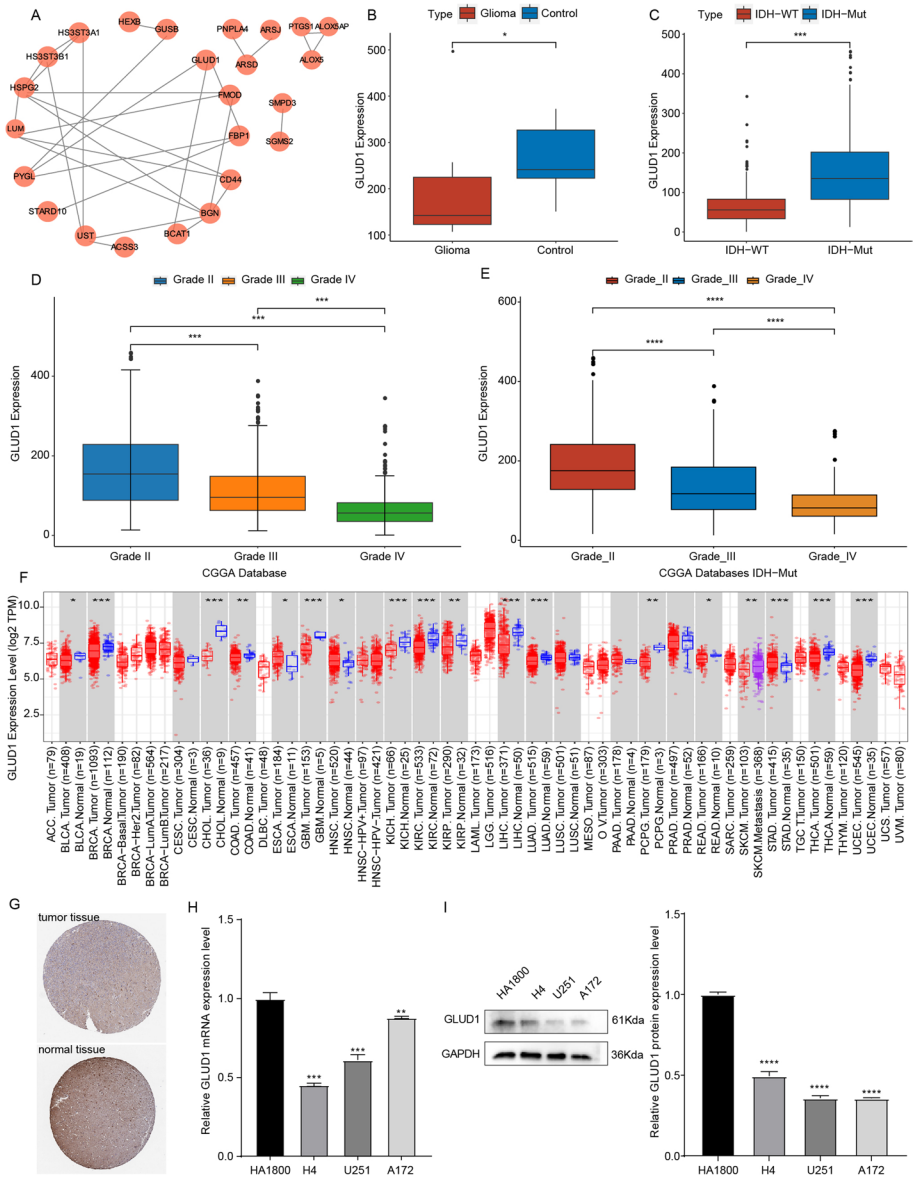

Fig. 2 The expression and survival analysis of GLUD1 in glioma patients. **A** PPI network of 34 candidate genes. **B** The expression of GLUD1 in GSE31095 dataset. **C** Expression of GLUD1 between IDH-mutant samples and IDH-wildtype samples. **D** The expression of GLUD1 in different histological grades. **D** Expression of GLUD1 between IDH-mutant samples and IDH-wildtype samples. **E** Expression of GLUD1 in IDH-mutant samples in different histological grades. **F** Expression of GLUD1 in various cancers. **G** Sections of GLUD1 expression in pathological and normal tissue from HPA database. **H** GLUD1 expression in glioma (H4, U251, and A172) and normal human astrocytes (HA1800) cell lines detected by qRT-PCR. **I** GLUD1 protein levels in glioma (H4, U251, and A172) and normal human astrocytes (HA1800) cell lines tested by WB. The grouping of blots were cropped from different gels

dataset. Samples were grouped into GLUD1^{high} and GLUD1^{low} groups based on the median value of GLUD1 expression. The results showed that 165 pathways were significantly enriched (p-value < 0.05). The top 20 pathways based on NES (normalized enrichment score) value were shown in Fig. 4A. The Calcium signaling pathway, MAPK signaling pathway, and other pathways were significantly enriched were shown in Fig. 4B. Furthermore, we divided the IDH-mutant samples into HGG and LGG groups and performed GSEA analysis on them respectively. The pathways activated in both groups were similar, such as Retrograde endocannabinoid signaling, GABAergic synapse, Wnt signaling pathway (Fig. 4C-F). DO enrichment analysis was performed on the DEGs and 203 pathways were significantly enriched (p-value < 0.05). The top 20 significantly

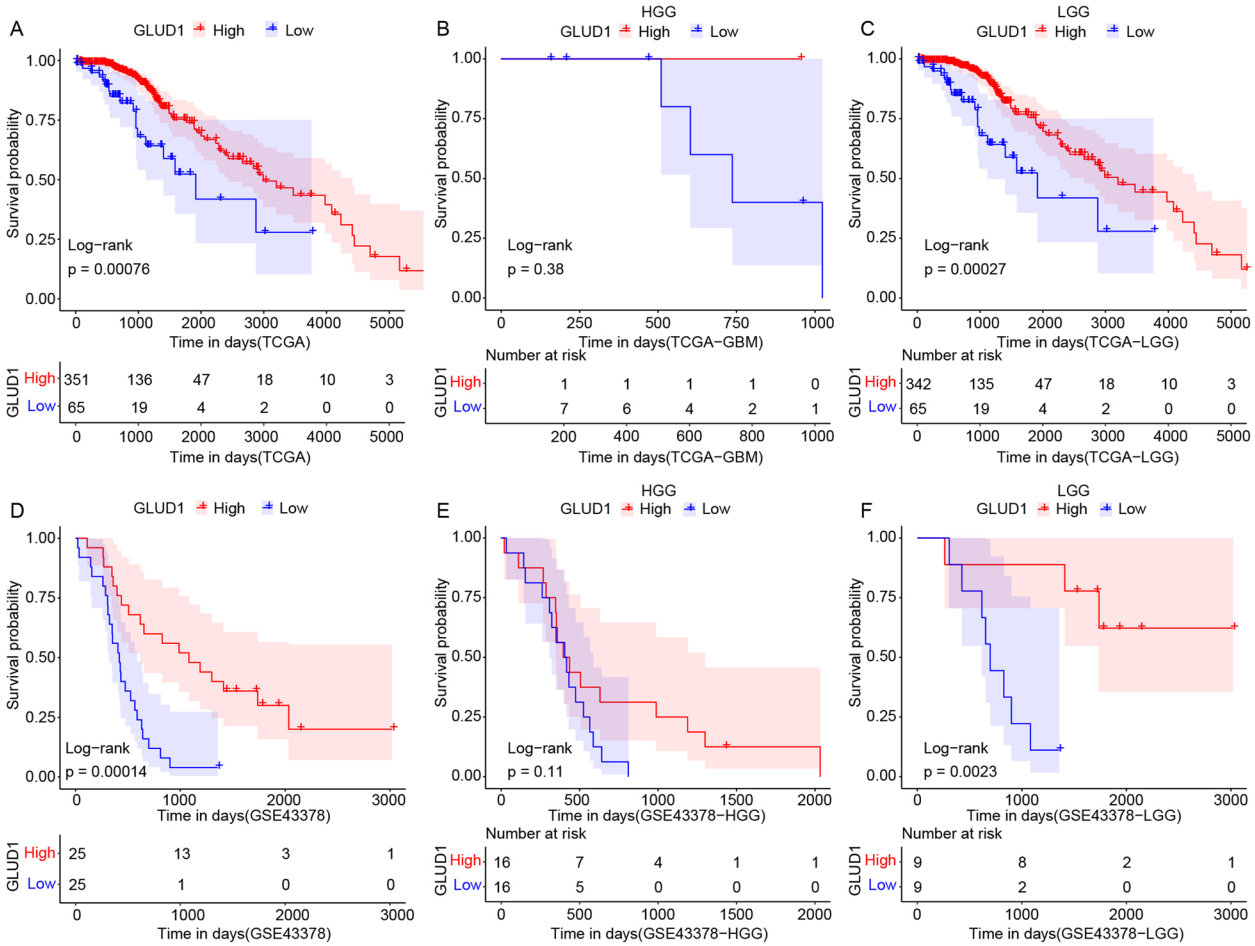

Fig. 3 KM survival analysis of IDH-mutant samples. **A**-**C** KM survival curves between different GLUD1 expression groups in IDH-mutant samples based on TCGA dataset, HGG and LGG samples. **D**-**F** KM survival curves between different GLUD1 expression groups in IDH-mutant samples based on GSE43378 dataset, HGG and LGG samples

enriched pathways were shown in Fig. 4G. The detailed results were summarized in Table S5.

Immune landscape in IDH-mutant glioma based on GLUD1 expression levels

Tumor microenvironment plays a vital role in the progression. The immune landscape aids a lot in exploring the underlying mechanisms and corresponding treatment. Using IDH-mutant glioma samples from TCGA, we analyzed the correlation between GLUD1 and the abundance of various immune-infiltrating cells using two databases, xCell and TISIDB. In xCell, seven immune cells, including regulatory T cells (Tregs), showed a significant positive correlation, while 25 immune cells, were significantly negatively correlated with GLUD1 ($p < 0.05$, Fig. 5A). In TISIDB, GLUD1 expression showed a significant positive correlation with five immune cells, including effector memory $CD4^+$ T cells (Tem_CD4), and a significant negative correlation with 10 immune cells, including activated $CD8^+$ T cells (Act_CD8) ($p < 0.05$, Fig. 5B, Table S6).

Based on the median expression level of the GLUD1 gene, we divided IDH-mutant glioma samples from TCGA into $GLUD1^{high}$ group and $GLUD1^{low}$ group. Then the differences in infiltration ratios of 22 types of immune cells between the two groups were analyzed. The results showed significant differences in eight types of immune cells ($CD8^+$ T cells, activated memory $CD4^+$ T cells, follicular helper T cells, regulatory T cells, resting NK cells, monocytes, activated dendritic cells, activated mast cells) between $GLUD1^{high}$ group and $GLUD1^{low}$ group (Fig. 5C). Subsequently, the same analysis was performed on HGG (TCGA-GBM) and LGG (TCGA-LGG) respectively. The significance was not available due to the small sample size of TCGA-GBM. The infiltration ratio of Tregs in HGG was lower in $GLUD1^{low}$ group but significantly higher in LGG $GLUD1^{low}$ group. In both HGG

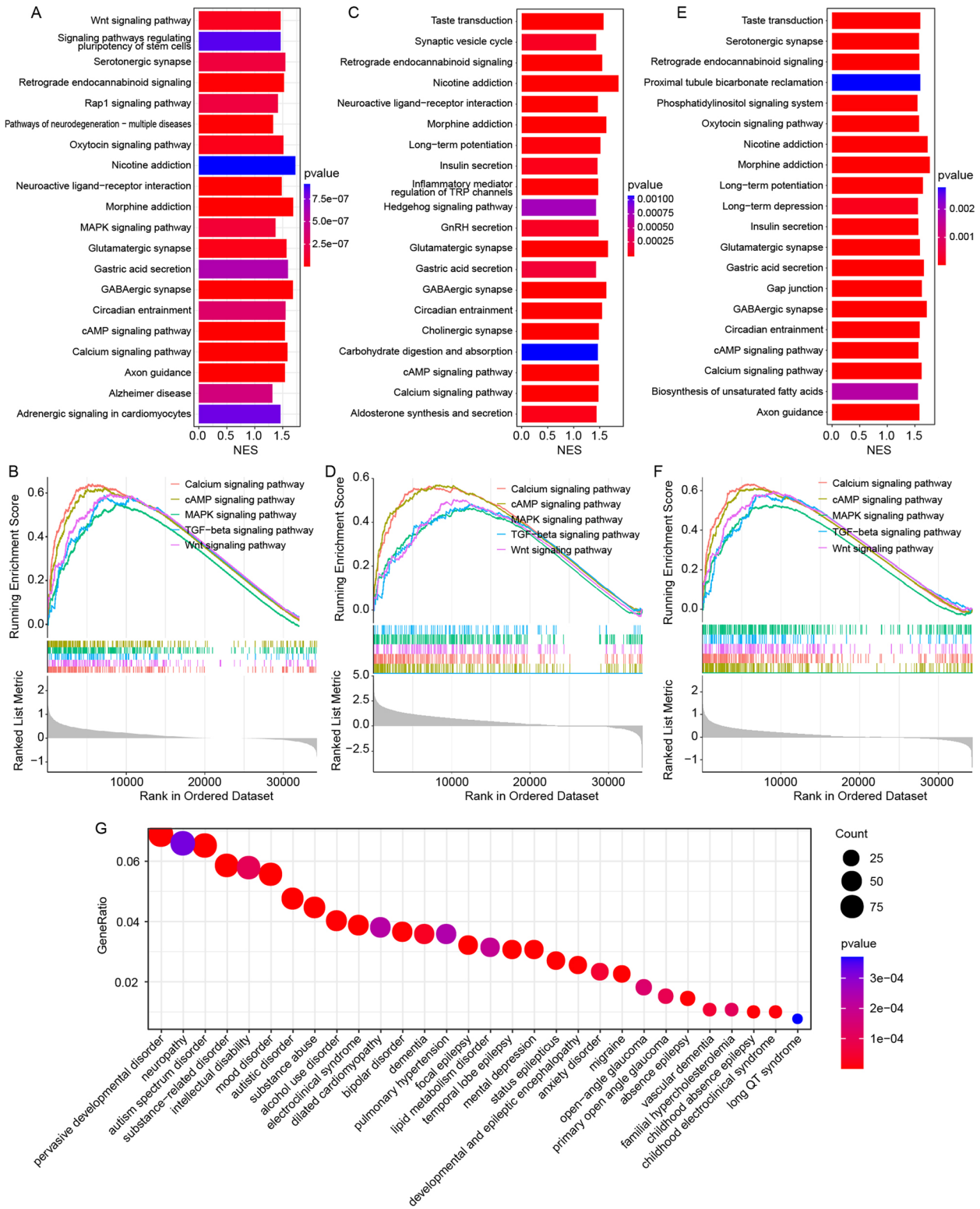

Fig. 4 GSEA and DO analysis of GLUD1 in IDH-mutant glioma samples. **A** GSEA analysis according to NES. **B** Five significantly enriched pathways in GSEA analysis. **C** GSEA analysis of IDH-mutant HGG glioma. **D** Five significantly enriched pathways in GSEA analysis of IDH-mutant HGG glioma. **E** GSEA analysis of IDH-mutant LGG glioma. **F** Five significantly enriched pathways in GSEA analysis of IDH-mutant LGG glioma. **G** DO analysis between different GLUD1 expression groups

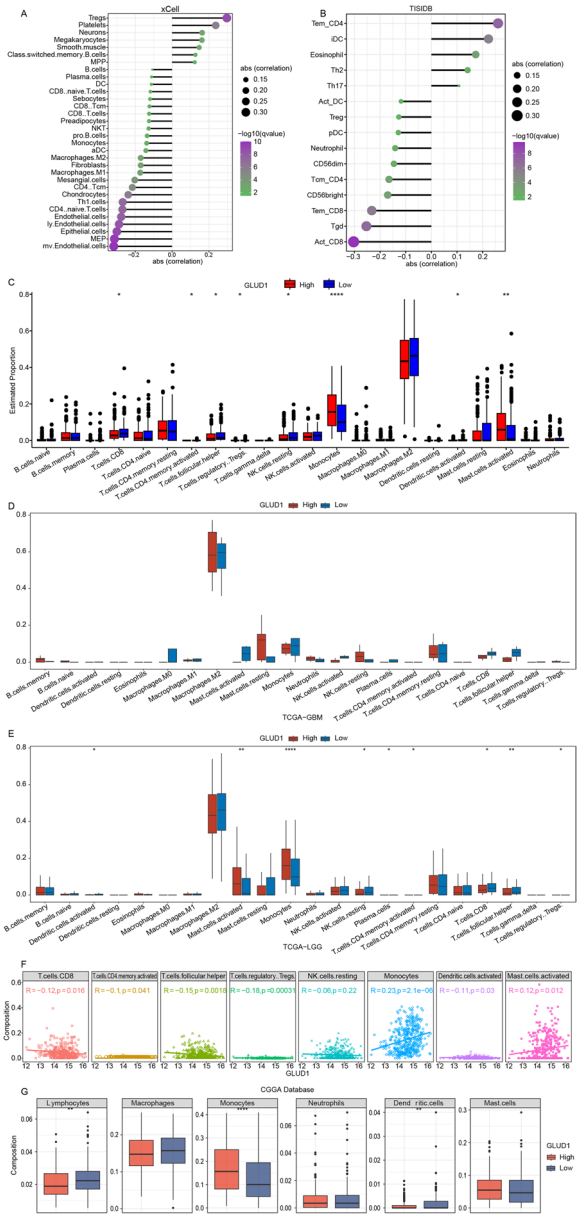

Fig. 5 Immune landscape of IDH-mutant glima samples. **A**-**B** Correlation of GLUD1 expression and the abundance of immune infiltrating cells in the xCell and TISIDB databases. **C** The infiltration ratios of 22 types of immune cells in GLUD1^{high} group and GLUD1^{low} group. **D**-**E** The infiltration ratios of 22 types of immune cells in GLUD1^{high} group and GLUD1^{low} group based on HGG and LGG samples, respectively. **F** Correlation between GLUD1 expression and 8 types of immune cells whose infiltration ratios were significantly different in GLUD1^{high} group and GLUD1^{low} group. **G** Differences in 6 categories of immune cells in GLUD1^{high} group and GLUD1^{low} group

and LGG, the proportions of plasma cells were higher in GLUD1^{low} group. Although the infiltration of plasma cells didn't show significance in all IDH-mutant samples (Fig. 5C), it showed significance in LGG (Fig. 5D-E). Among these immune cells, further analysis of Pearson correlation showed significant negative correlation with CD8^{+} T cells, activated memory CD4^{+} T cells, follicular helper T cells, regulatory T cells, and activated dendritic cells (p-value < 0.05), significant positive correlation with monocytes and activated mast cells (p-value < 0.05), and no significant correlation with resting NK cells (Fig. 5F).

Furthermore, the 22 types of immune cells were divided into six categories: Lymphocytes, Macrophages, Monocytes, Neutrophils, Dendritic cells, and Mast cells. Differences in the infiltration ratios of the six immune cell categories between GLUD1^{high} and GLUD1^{low} groups showed that the infiltration ratio of Monocytes was higher in GLUD1^{high} group, while Lymphocytes and Dendritic cells were higher in GLUD1^{low} group, and there was no significant difference in the other three categories between the two groups (Fig. 5 G).

Using IDH-mutant glioma samples from the CGGA database, we calculated the immune scores of the samples and ESTIMATEScore, ImmuneScore, and StromalScore were significantly higher in GLUD1^{low} group than GLUD1^{high} group, while TumorPurity was significantly lower in GLUD1^{low} group than GLUD1^{high} group (Fig. 6A).

We also performed single-sample gene set enrichment analysis ssGSEA analysis on IDH-mutant glioma samples from the CGGA database to further analyze the activity of immune cells. Immune cells were divided into innate immunity and adaptive immunity groups, and we found that the expression levels of both groups were significantly higher in GLUD1^{low} group than GLUD1^{high} group (Fig. 6B). Among adaptive immune cells, we divided them into T cell response and other cells, and found that tumors with low expression of GLUD1 elicited a relatively stronger T cell response (Fig. 6C).

Clinical outcomes of GLUD1 low expression IDH mutant glioma patients were poor

Clinical outcomes research can provide valuable insights into disease progression, survival rates, quality of life, and safety of medical interventions. In this study, KM survival analysis was performed on the samples in GLUD1^{high} group and GLUD1^{low} group. The results showed that patients in GLUD1^{low} group had a relatively low survival rate (Fig. 7A), and so were PFS (progression-free survival) as well as DFS (disease-free survival) (Fig. 7B-C).

Multivariate Cox regression analysis was performed on IDH-mutant glioma samples in the CGGA database, including Age and Gender. The results showed that the GLUD1 was an independent protective factor (hazard ratio < 1) for IDH-mutant glioma patients (Fig. 7D). Time-dependent receiver operating characteristic (ROC) analysis showed that the combined AUC (area under the ROC curve) of 1-year, 3-year, and 5-year survival periods

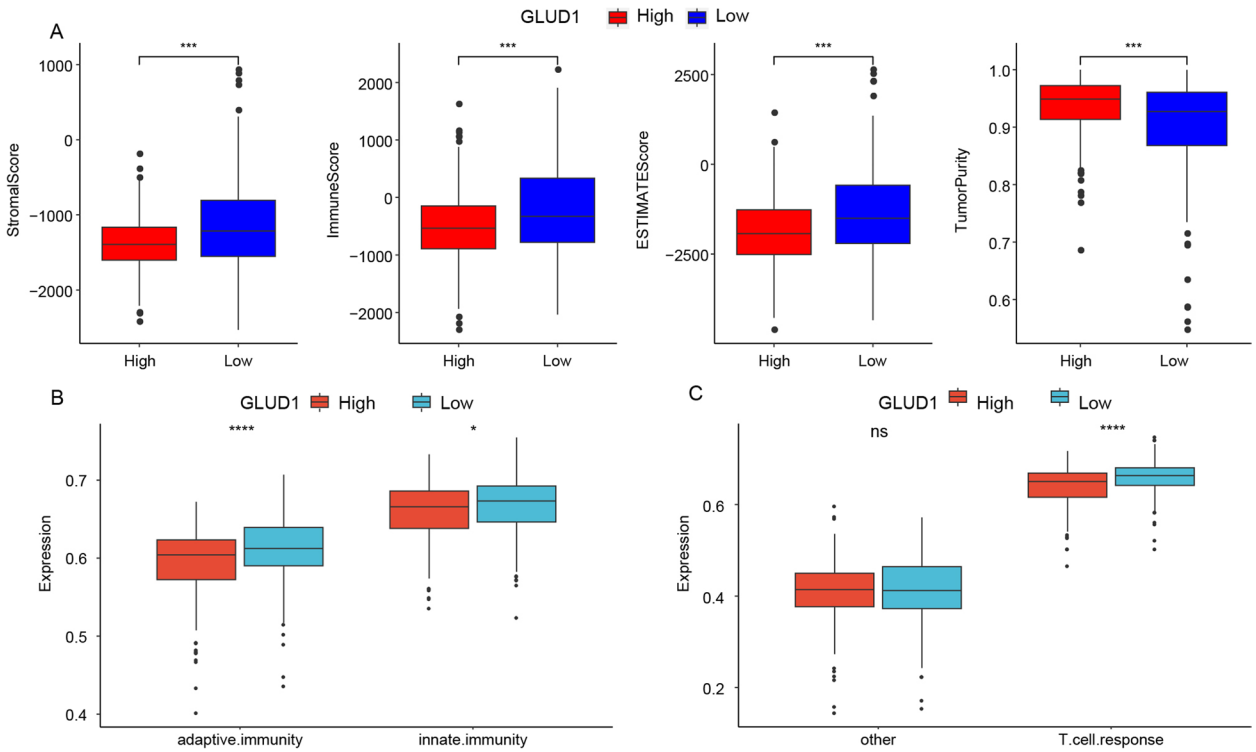

Fig. 6 **A** ImmuneScore, ESTIMATEScore, StromalScore and TumorPurity of samples in GLUD1^{high} group and GLUD1^{low} group. **B** Differences between innate immunity and adaptive immunity in GLUD1^{high} group and GLUD1^{low} group. **C** T cell response in GLUD1^{high} group and GLUD1^{low} group

were 0.71, 0.71, and 0.66, respectively, indicating that the GLUD1 can effectively predict the prognosis of IDH-mutant glioma patients (Fig. 7E).

Drug sensitivity research is helpful in developing personalized treatment plans for individual patients, which can improve treatment outcomes and minimize the risk of adverse drug reactions. Using IDH-mutant glioma samples in the CGGA database, the correlation between GLUD1 expression and the IC50 (half maximal inhibitory concentration) of drugs was analyzed, and the results showed that GLUD1 was significantly positively correlated with 11 drugs such as Dasatinib_1079, GSK269962A_1192, and Entospletinib_1630; and significantly negatively correlated with 108 drugs such as ML323_1629, GSK343_1627, and Sorafenib_1085 (p-value < 0.05, Fig. 7F, Table S7). For drugs with significant correlations, the differences in IC50 values between GLUD1^{high} group and GLUD1^{low} group were compared, and some results showed that Cediranib_1922, Ruxolitinib_1507, Doramapimod_1042, AZD1208_1449, Nelarabine_1814, and Dihydrorotenone_1827 were higher in GLUD1^{low} group (Fig. 7G).

The function of immune checkpoint genes is pivotal to the efficacy of immunotherapy. Expression differences of six immune checkpoint genes (PD-1 (PDCD1), CTLA4, PDL-1 (CD274), CD80, LAG3, TIGIT) were compared between GLUD1^{high} group and GLUD1^{low} group, and the results showed that the expression levels of the PDCD1, CTLA4, CD80, and LAG3 genes were significantly lower in GLUD1^{high} group, suggesting the expression of GLUD1 was associated with immune microenvironment (Fig. 7H).

Discussion

In this study, we conducted a screening of 34 energy metabolism-related genes functioning in glioma, with the objective of identifying a target gene. Following this screening process, we selected GLUD1 as the target gene. It showed higher expression in IDH-mutant and normal samples than in IDH-wildtype and tumor samples. Low expression was associated with poor prognosis, and stronger T cell responses. Our results demonstrated that GLUD1 was an independent prognostic indicator for IDH-mutant glioma.

The GLUD1 (glutamate dehydrogenase (GDH) 1) which includes 13 exons is involved in the metabolism of glutamate [26]. This gene is situated on chromosome 10q23.3 and is predominantly expressed in the liver, pancreas, and brain [27]. GDH plays a critical role in the regulation of not only glutamine metabolism but also

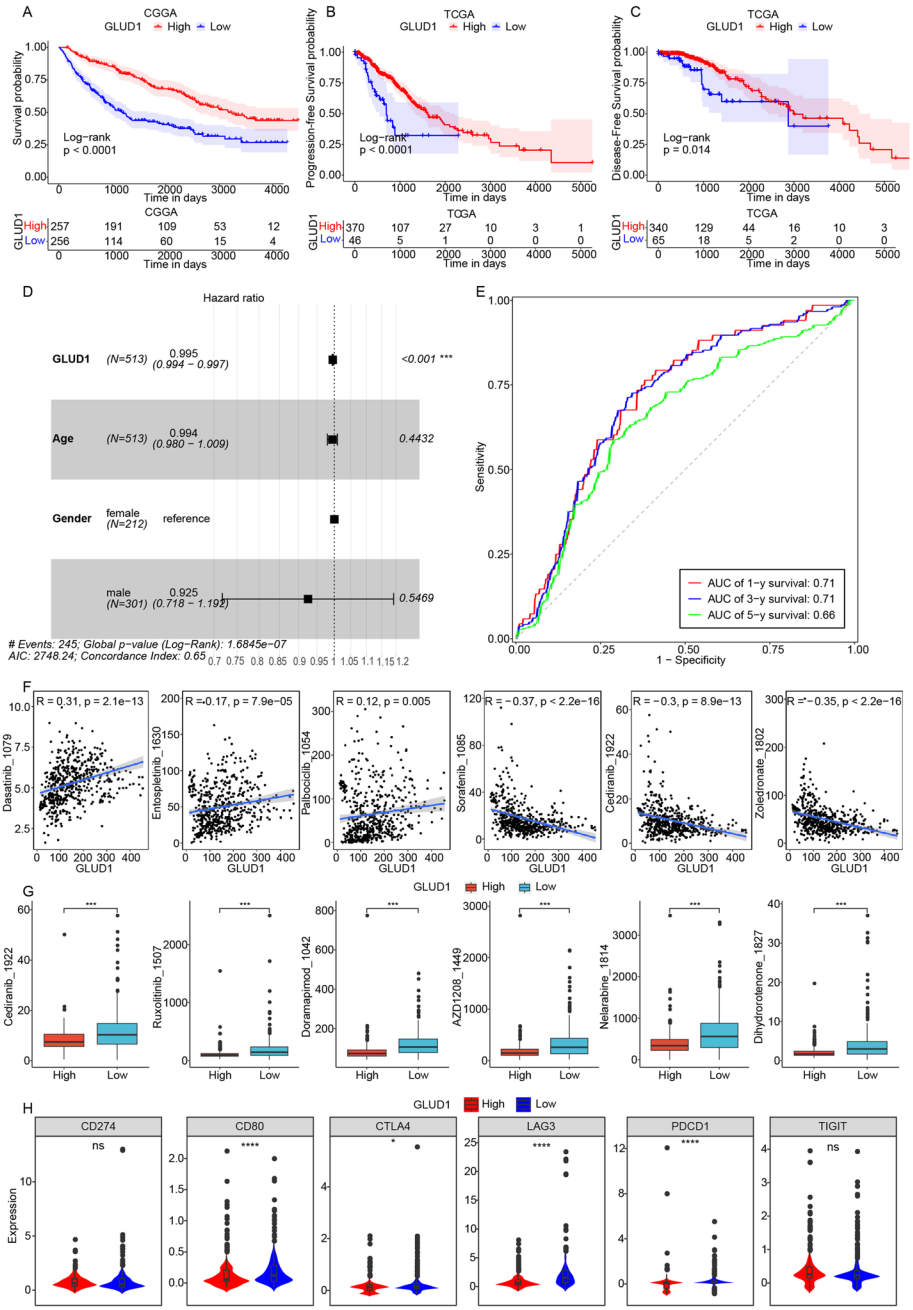

Fig. 7 Clinical outcome of IDH mutant glioma patients based on GLUD1 expression. **A** Kaplan Meier survival curves of GLUD1^{high} group and GLUD1^{low} group in CGGA dataset. **B**-**C** PFS and DFS survival curves of GLUD1^{high} group and GLUD1^{low} group in TCGA dataset. **D** Multivariate Cox regression analysis. **E** ROC curve of GLUD1. **F** Correlation between GLUD1 expression and drug sensitivity. **G** Differences in IC50 levels between GLUD1^{high} group and GLUD1^{low} group of drugs with significant correlation. **H** 6 immune checkpoint gene expression in GLUD1^{high} group and GLUD1^{low} group

cellular energy metabolism by controlling the flow of carbon and nitrogen between amino acids and the tricarboxylic acid cycle [28]. GLUD1 has been demonstrated to influence the progression of a number of cancers, including breast and lung cancers [29, 30]. The findings of our study indicate that GLUD1 plays a role in glioma, with higher expression levels associated with a more favourable prognosis. The expression level of GLUD1 gradually decreased as the grade was processed in glioma. The same pattern was observed in clear cell renal cell

carcinoma [31]. GLUD1 expression was found to be significantly reduced in bladder urothelial carcinoma, breast invasive carcinoma, and other tumor samples according to TIMER database. In triple-negative breast cancer, high GLUD1 expression was associated with a better outcome in patients treated with chemotherapy [32]. The results of GSEA and DO analysis indicated that GLUD1 might influence a lot of neurological diseases, such as neuropathy, autism spectrum disorder, Alzheimer's disease, intellectual disability, substance abuse, etc. Deregulation of human GDHs (encoded by GLUD) has been linked to the development of neurological disorders, for instances, epileptic seizures, generalized dystonia, and mental retardation [33]. The anaplerotic function of GDH1 (encoded by GLUD1) has attracted much attention due to its vital role in glioma [34]. A lot of pathways functioned when GLUD1 worked in the process of IDH-mutant glioma, such as MAPK signaling pathway, Calcium signaling pathway, and cAMP signaling pathways.

The infiltration of immune cells in IDH-mutant glioma, and it was found that $CD8^+$ T cells, activated memory $CD4^+$ T cells, follicular helper T cells, regulatory T cells, and activated dendritic cells were significantly negatively correlated to GLUD1 expression. Conversely, monocytes and activated mast cells were significantly positively correlated to GLUD1 expression. GLUD1 and GLUD2 are δ receptors in mast cells [35]. GLUD1 is capable of controlling autophagy, and further regulating the malignant conditions of tumors [36, 37]. When monocytes are ready to differentiate, autophagy is induced, and induction is critical for the monocytes' survival and differentiation. On the contrary, inhibition of autophagy leads to apoptosis of monocytes involved in differentiation [38]. It can be surmised that the differentiation from monocytes to macrophages may be inhibited by GLUD1. In IDH-mutant samples, ESTIMATEScore, ImmuneScore, and StromalScore were significantly higher in $GLUD1^{low}$ group than $GLUD1^{high}$ group. A total of 11 drugs demonstrated a significant positive correlation with GLUD1 expression, while 108 drugs exhibited a significant negative correlation. 6 immune checkpoint genes were also significantly differentially expressed in $GLUD1^{high}$ group and $GLUD1^{low}$ group. The results showed GLUD1's potential in glioma treatment. GLUD1 inhibits cancer cells' proliferation and migration, and it is a target for cancer therapy, for example, combination therapy of anticancer drugs adding a GLUD1 inhibitor is effective [39].

Conclusions

This study focused on identifying energy metabolism-related genes in glioma and selected GLUD1 as the target gene, finding that GLUD1 expression was higher in IDH-mutant samples than in IDH-wildtype samples and that lower expression was associated with poor prognosis. Furthermore, our findings indicated that GLUD1 played a role in shaping distinct immune microenvironment in IDH-mutant glioma. Additionally, GLUD1 expression was related to several drugs and immune checkpoint genes. The findings of our study offer valuable insights for the development of immunotherapy for IDH-mutant glioma.

Supplementary Information

The online version contains supplementary material available at https://doi.org/10.1186/s12883-024-03787-w.

Supplementary Material 1. Table S1. 1384 energy metabolism-related genes.

Supplementary Material 2. Table S2. 179 differentially expressed energy metabolism-related genes.

Supplementary Material 3. Table S3. 34 candidate genes.

Supplementary Material 4. Table S4. KEGG and GO enrichment analysis.

Supplementary Material 5. Table S5. GSEA and DO enrichment analysis.

Supplementary Material 6. Table S6. Correlation between GLUD1 expression and infiltration ratios of immune cells from xCell and TISIDB databases.

Supplementary Material 7. Table S7. Correlation between GLUD1 expression and drug sensitivity.

Supplementary Material 8.

Acknowledgements
Not applicable.

Authors' contributions
RZ.D. and XY.S. conceived the study; RZ.D., L.W. and DD.Z. guided the methods; RZ.D., JY.Q., L.W. and DD.Z. conducted the software; RZ.D., HB.L., N.W., K.Q., JH.D. and JH.W. validated the study; RZ.D., JY.Q., L.W. and DD.Z. analyzed the data; RZ.D. and L.W. investigated the research; RZ.D., HB.L., N.W., K.Q., JH.D. and JH.W. prepared for the resources; RZ.D., JY.Q., L.W., DD.Z., HB.L. and N.W. collected the data; RZ.D. drafted the original manuscript; RZ.D. and XY.S. reviewed and edited the article; RZ.D. visualized the study; XY.S. and RZ.D. supervised the research; XY.S. and RZ.D. administrated the project. All authors read and approved the final manuscript.

Funding
The authors did not receive support from any organization for the submitted work.

Availability of data and materials
The mRNA expression profiles and corresponding clinical information are from The Cancer Genome Atlas (TCGA) database [https://portal.gdc.cancer.gov/] for TCGA-LGG and TCGA-GBM patients. The mRNA expression profiles and clinical information of 1018 patients are from the Chinese Glioma Genome Atlas (CGGA) database [http://www.cgga.org.cn/] for CGGA-693 and CGGA-325 datasets. The datasets GSE131273, GSE4290, GSE43378, and GSE31095) are from the Gene Expression Omnibus (GEO) database [https://www.ncbi.nlm.nih.gov/geo/].

Data availability
No datasets were generated or analysed during the current study.

Declarations

Ethics approval and consent to participate
Not applicable.

Consent for publication
Not applicable.

Competing interests
The authors declare no competing interests.

Received: 17 November 2023 Accepted: 30 July 2024
Published online: 13 September 2024

References

1. Ostrom QT, Gittleman H, Liao P, Rouse C, Chen Y, Dowling J, et al. CBTRUS statistical report: primary brain and central nervous system tumors diagnosed in the United States in 2007–2011. Neuro Oncol. 2014;16(Suppl 4):iv1-63. https://doi.org/10.1093/neuonc/nou223.
2. Hsu SPC, Lin MH, Lin CF, Hsiao TY, Wang YM, Sun CW. Brain tumor grading diagnosis using transfer learning based on optical coherence tomography. Biomed Opt Express. 2024;15(4):2343–57. https://doi.org/10.1364/BOE.513877.
3. Bai H, Harmanci AS, Erson-Omay EZ, Li J, Coskun S, Simon M, et al. Integrated genomic characterization of IDH1-mutant glioma malignant progression. Nat Genet. 2016;48(1):59–66. https://doi.org/10.1038/ng.3457.
4. Ohba S, Mukherjee J, See WL, Pieper RO. Mutant IDH1-driven cellular transformation increases RAD51-mediated homologous recombination and temozolomide resistance. Cancer Res. 2014;74(17):4836–44. https://doi.org/10.1158/0008-5472.CAN-14-0924.
5. Hanahan D, Weinberg RA. Hallmarks of cancer: the next generation. Cell. 2011;144(5):646–74. https://doi.org/10.1016/j.cell.2011.02.013.
6. Pearl, H. and C. C. Fleischer, Association between altered metabolism and genetic mutations in human glioma. Cancer Rep (Hoboken). 2023:e1799. https://doi.org/10.1002/cnr2.1799.
7. Ohshima, K. and E. Morii, Metabolic reprogramming of cancer cells during tumor progression and metastasis. Metabolites. 2021; 11(1) https://doi.org/10.3390/metabo11010028.
8. Al-Khallaf H. Isocitrate dehydrogenases in physiology and cancer: biochemical and molecular insight. Cell Biosci. 2017;7:37. https://doi.org/10.1186/s13578-017-0165-3.
9. Yen KE, Bittinger MA, Su SM, Fantin VR. Cancer-associated IDH mutations: biomarker and therapeutic opportunities. Oncogene. 2010;29(49):6409–17. https://doi.org/10.1038/onc.2010.444.
10. Krell D, Assoku M, Galloway M, Mulholland P, Tomlinson I, Bardella C. Screen for IDH1, IDH2, IDH3, D2HGDH and L2HGDH mutations in glioblastoma. PLoS ONE. 2011;6(5):e19868. https://doi.org/10.1371/journal.pone.0019868.
11. Parsons DW, Jones S, Zhang X, Lin JC, Leary RJ, Angenendt P, et al. An integrated genomic analysis of human glioblastoma multiforme. Science. 2008;321(5897):1807–12. https://doi.org/10.1126/science.1164382.
12. Huang J, Yu J, Tu L, Huang N, Li H, Luo Y. Isocitrate dehydrogenase mutations in glioma: from basic discovery to therapeutics development. Front Oncol. 2019;9:506. https://doi.org/10.3389/fonc.2019.00506.
13. Yan H, Parsons DW, Jin G, Mclendon R, Rasheed BA, Yuan W, et al. IDH1 and IDH2 mutations in gliomas. N Engl J Med. 2009;360(8):765–73. https://doi.org/10.1056/NEJMoa0808710.
14. Laurentino, T. S., R. D. S. Soares, S. K. N. Marie, and S. M. Oba-Shinjo, Correlation of Matrisome-Associatted Gene Expressions with LOX Family Members in Astrocytomas Stratified by IDH Mutation Status. Int J Mol Sci. 2022; 23(17). https://doi.org/10.3390/ijms23179507.
15. Chan AK, Yao Y, Zhang Z, Shi Z, Chen L, Chung NY, et al. Combination genetic signature stratifies lower-grade gliomas better than histological grade. Oncotarget. 2015;6(25):20885–901. https://doi.org/10.18632/oncotarget.4928.
16. Wang L, Li X. Identification of an energy metabolism-related gene signature in ovarian cancer prognosis. Oncol Rep. 2020;43(6):1755–70. https://doi.org/10.3892/or.2020.7548.
17. Ritchie ME, Phipson B, Wu D, Hu Y, Law CW, Shi W, et al. limma powers differential expression analyses for RNA-sequencing and microarray studies. Nucleic Acids Res. 2015;43(7):e47. https://doi.org/10.1093/nar/gkv007.
18. Yu G, Wang LG, Han Y, He QY. clusterProfiler: an R package for comparing biological themes among gene clusters. OMICS. 2012;16(5):284–7. https://doi.org/10.1089/omi.2011.0118.
19. Szklarczyk D, Gable AL, Lyon D, Junge A, Wyder S, Huerta-Cepas J, et al. STRING v11: protein-protein association networks with increased coverage, supporting functional discovery in genome-wide experimental datasets. Nucleic Acids Res. 2019;47(D1):D607–13. https://doi.org/10.1093/nar/gky1131.
20. Shannon P, Markiel A, Ozier O, Baliga NS, Wang JT, Ramage D, et al. Cytoscape: a software environment for integrated models of biomolecular interaction networks. Genome Res. 2003;13(11):2498–504. https://doi.org/10.1101/gr.1239303.
21. Maeser, D., R. F. Gruener, and R. S. Huang, oncoPredict: an R package for predicting in vivo or cancer patient drug response and biomarkers from cell line screening data. Brief Bioinform. 2021; 22(6). https://doi.org/10.1093/bib/bbab260.
22. Boer JC, Van Marion DM, Joseph JV, Kliphuis NM, Timmer-Bosscha H, Van Strijp JA, et al. Microenvironment involved in FPR1 expression by human glioblastomas. J Neurooncol. 2015;123(1):53–63. https://doi.org/10.1007/s11060-015-1777-2.
23. Yu G, Wang LG, Yan GR, He QY. DOSE: an R/Bioconductor package for disease ontology semantic and enrichment analysis. Bioinformatics. 2015;31(4):608–9. https://doi.org/10.1093/bioinformatics/btu684.
24. Newman AM, Liu CL, Green MR, Gentles AJ, Feng W, Xu Y, et al. Robust enumeration of cell subsets from tissue expression profiles. Nat Methods. 2015;12(5):453–7. https://doi.org/10.1038/nmeth.3337.
25. Michaelis EK, Wang X, Pal R, Bao X, Hascup KN, Wang Y, et al. Neuronal Glud1 (glutamate dehydrogenase 1) over-expressing mice: increased glutamate formation and synaptic release, loss of synaptic activity, and adaptive changes in genomic expression. Neurochem Int. 2011;59(4):473–81. https://doi.org/10.1016/j.neuint.2011.03.003.
26. Deloukas P, Dauwerse JG, Moschonas NK, Van Ommen GJ, Van Loon AP. Three human glutamate dehydrogenase genes (GLUD1, GLUDP2, and GLUDP3) are located on chromosome 10q, but are not closely physically linked. Genomics. 1993;17(3):676–81. https://doi.org/10.1006/geno.1993.1389.
27. Hudson RC, Daniel RM. L-glutamate dehydrogenases: distribution, properties and mechanism. Comp Biochem Physiol B. 1993;106(4):767–92. https://doi.org/10.1016/0305-0491(93)90031-y.
28. Plaitakis, A., E. Kalef-Ezra, D. Kotzamani, I. Zaganas, and C. Spanaki. The glutamate dehydrogenase pathway and its roles in cell and tissue biology in health and disease. Biology (Basel). 2017; 6(1). https://doi.org/10.3390/biology6010011.
29. Wu YJ, Hu ZL, Hu SD, Li YX, Xing XW, Yang Y, et al. Glutamate dehydrogenase inhibits tumor growth in gastric cancer through the Notch signaling pathway. Cancer Biomark. 2019;26(3):303–12. https://doi.org/10.3233/CBM-190022.
30. Coloff JL, Murphy JP, Braun CR, Harris IS, Shelton LM, Kami K, et al. Differential glutamate metabolism in proliferating and quiescent mammary epithelial cells. Cell Metab. 2016;23(5):867–80. https://doi.org/10.1016/j.cmet.2016.03.016.
31. Wang L, Fang Z, Gao P, Zheng J. GLUD1 suppresses renal tumorigenesis and development via inhibiting PI3K/Akt/mTOR pathway. Front Oncol. 2022;12:975517. https://doi.org/10.3389/fonc.2022.975517.
32. Craze ML, El-Ansari R, Aleskandarany MA, Cheng KW, Alfarsi L, Masisi B, et al. Glutamate dehydrogenase (GLUD1) expression in breast cancer. Breast Cancer Res Treat. 2019;174(1):79–91. https://doi.org/10.1007/s10549-018-5060-z.
33. Plaitakis A, Zaganas I, Spanaki C. Deregulation of glutamate dehydrogenase in human neurologic disorders. J Neurosci Res. 2013;91(8):1007–17. https://doi.org/10.1002/jnr.23176.
34. Spanaki C, Kotzamani D, Plaitakis A. Widening Spectrum of Cellular and Subcellular Expression of Human GLUD1 and GLUD2 Glutamate Dehydrogenases Suggests Novel Functions. Neurochem Res. 2017;42(1):92–107. https://doi.org/10.1007/s11064-016-1986-x.
35. Rouadi PW, Idriss SA, Bousquet J, Laidlaw TM, Azar CR, Sulaiman Al-Ahmad M, et al. WAO-ARIA consensus on chronic cough - Part 1: Role of TRP channels in neurogenic inflammation of cough neuronal pathways. World Allergy Organ J. 2021;14(12):100617. https://doi.org/10.1016/j.waojou.2021.100617.

36. Lorin S, Tol MJ, Bauvy C, Strijland A, Pous C, Verhoeven AJ, et al. Glutamate dehydrogenase contributes to leucine sensing in the regulation of autophagy. Autophagy. 2013;9(6):850–60. https://doi.org/10.4161/auto.24083.
37. Deberardinis RJ, Lum JJ, Hatzivassiliou G, Thompson CB. The biology of cancer: metabolic reprogramming fuels cell growth and proliferation. Cell Metab. 2008;7(1):11–20. https://doi.org/10.1016/j.cmet.2007.10.002.
38. Zhang Y, Morgan MJ, Chen K, Choksi S, Liu ZG. Induction of autophagy is essential for monocyte-macrophage differentiation. Blood. 2012;119(12):2895–905. https://doi.org/10.1182/blood-2011-08-372383.
39. Wang Q, Wu M, Li H, Rao X, Ao L, Wang H, et al. Therapeutic targeting of glutamate dehydrogenase 1 that links metabolic reprogramming and Snail-mediated epithelial-mesenchymal transition in drug-resistant lung cancer. Pharmacol Res. 2022;185:106490. https://doi.org/10.1016/j.phrs.2022.106490.

Publisher's Note